Catalysis Today 232 (2014) 127–133

Contents lists available at ScienceDirect

Catalysis Today

journal homepage: www.elsevier.com/locate/cattod

Catalytic performance of ion-exchanged montmorillonite with quaternary ammonium salts for the glycerolysis of urea

Sun-Do Lee[a], Moon-Seok Park[a], Dong-Woo Kim[a], Il Kim[b], Dae-Won Park[a,*]

[a] School of Chemical and Biomolecular Engineering, Pusan National University, Busan 609-735, Republic of Korea
[b] Department of Polymer Science and Engineering, Pusan National University, Busan 609-735, Republic of Korea

ARTICLE INFO

Article history:
Received 10 July 2013
Received in revised form 26 August 2013
Accepted 2 October 2013
Available online 28 October 2013

Keywords:
Glycerol
Glycerol carbonate
Ion-exchange method
Montmorillonite
Quaternary ammonium salt
Urea

ABSTRACT

Various quaternary ammonium salt (QX) ionic liquids immobilized onto montmorillonite clay (Q-MMT) were prepared by ion-exchange reaction between the tetra-alkyl ammonium salts and ions in the clay interlayer. The Q-MMTs were characterized by elemental analyses, nitrogen adsorption–desorption, XRD, ^{13}C and ^{27}Al NMR, TGA, FT-IR, and HRTEM. The *d*-spacing of the Q-MMTs increased with increasing alkyl chain lengths, however, the surface areas decreased by immobilizing QX onto MMTs. The Q-MMTs showed good catalytic activity for the synthesis of glycerol carbonate from glycerol and urea. The effects of the ionic liquid cation structure, and reaction parameters, such as temperature and degree of vacuum, on the performance of Q-MMTs were also discussed. The catalyst could be reused in up to four consecutive runs without any considerable loss of activity.

1. Introduction

The biodiesel has proved its value as a fuel for diesel engines and is renewable and clean [1–3]. Due to the rapid increase in the use of biodiesel and the sharp decrease in glycerol prices, glycerol has the potential to become a major platform chemical and has been identified as an important building block for future biorefineries by the DOE [4]. Glycerol carbonate (GC), which can be synthesized from glycerol, is a new and interesting material in the chemical industry [5]. It attracts much attention because of its low toxicity, good biodegradability, and high boiling point. It has been investigated as a novel component of gas separation membranes, polyurethane foams [6], a surfactant component [7], a nonvolatile reactive solvent for several types of materials, and a component in coatings, paints, and detergents.

The main methods for the preparation of GC involve the reaction of glycerol with (a) a carbon source (phosgene, a dialkyl carbonate, or an alkylene carbonate), (b) carbon monoxide and oxygen or carbon dioxide, or (c) urea. Traditionally, GC has been prepared by the reaction of glycol with phosgene; however, because of the high toxicity and corrosive nature of phosgene, alternative preparative methods for GC, such as glycerolysis of urea, have been explored [8–10].

The major advantage of the glycerolysis of urea is that the reactant, urea, is readily available and inexpensive. In addition, the ammonia formed can be easily converted to urea in the presence carbon dioxide. Several catalysts have been used, mainly based on metal oxides of variable basicity [8–10]. However, these catalysts are difficult to separate from the reaction mixture, because they dissolve in the reactants or are converted into micropowders.

Montmorillonite (MMT) is a 2:1 layer mineral of hydrated aluminum silicate, where the anionic charge of the aluminosilicate layer is neutralized by the intercalation of compensating, exchangeable cations (e.g., Na^+, Ca^{2+}, and Mg^{2+}), and their coordinated water molecules. Montmorillonites are highly reactive with a variety of organic molecules interacting through electrostatic interactions (e.g., ion exchange), secondary bonding (e.g., adsorption of neutral species), or covalent bonding (e.g., grafting) to produce novel compounds [11,12]. The interactions of MMTs with different organic molecules have been reviewed by Ruiz-Hitzky et al. [13]. In the modification of MMTs by ion exchange, the interlayer-accessible compensating cations can be exchanged with a wide variety of hydrated inorganic or organic cations including those of amines or quaternary ammonium salts, as well as oxonium, sulfonium, phosphonium, and more complex cationic species such as methylene blue and cationic dyestuffs [11,14,15]. Important incentives were the improvement of the thermal stabilities of the organoclays and the preparation of nanocomposites with enhanced flame retardant characteristics. However, only limited work has been reported for the

* Corresponding author. Tel.: +82 51 510 2399; fax: +82 51 512 8563.
E-mail address: dwpark@pusan.ac.kr (D.-W. Park).

0920-5861/$ – see front matter © 2013 Elsevier B.V. All rights reserved.
http://dx.doi.org/10.1016/j.cattod.2013.10.009

catalytic applications of the ionic liquids (ILs) immobilized on MMT [16].

Ionic liquids are proven to be environmentally benign media for catalytic processes or chemical extraction [17]. ILs have negligible vapor pressure, excellent thermal stability, and special characteristics as opposed to conventional organic and inorganic solvents. Quaternary ammonium salts are some of typical ILs. They can be widely used as catalysts in many organic syntheses [18–20].

We studied the performance of immobilized ILs on MCM-41 or Merrifield peptide resin for the synthesis of GC [21,22]. However, the use of expensive pore-directing agents and large amounts of organic solvents for template removal make these catalysts impractical for commercial production. Moreover, the ordering of the mesopores often decreases because of the use of such agents and solvents. These findings emphasize the need for a low-cost and commercially viable type of clay as a support.

In this study, ammonium salt type ILs were ion-exchanged with a commercial MMT to investigate the performance of this heterogeneous catalyst in the synthesis of GC from glycerol and urea. The effects of the ionic liquid cation structure, reaction time, temperature, and degree of vacuum are discussed for a better understanding of the reaction mechanism. A recycle test of Q-MMT was also performed to assess the stability of the catalyst.

2. Experimental procedures

2.1. Materials

Na^+-MMT, a hydrated aluminum silicate with sodium as the predominant exchangeable cation (trade name: Kunipia-F, Kunimine Industrial Company), is obtained in powder form with a typical particle size of less than 2 μm. The cation exchange capacity (CEC) of Na^+-MMT, as reported by the supplier, is 120 mequiv./100 g clay and the pH value of a 10% aqueous suspension is 10. Ionic liquids are used for the modification of MMT by ion exchange, which included tetrabutylammonium chloride (TBAC), tetrahexylammonium chloride (THAC), tetraoctylammonium chloride (TOAC), and tetradodecylammonium chloride (TDAC). They were obtained from Sigma–Aldrich and were used as obtained.

2.2. Preparation of Q-MMT

Quaternary ammonium salts embedded MMT hybrids (referred to hereafter as Q-MMT) with different alkyl chain lengths were prepared by the ion-exchange method. In a 250-mL beaker, MMT-Na^+ (1.0 g, 1.2 mequiv./g) was placed and 100-mL deionized water was added. The mixture was vigorously stirred with a magnetic stirrer and heated to 30 °C to obtain a swollen Na^+-MMT slurry. In a separate vessel, the quaternary ammonium salts (QX, 1.2 mmol) were dissolved in 20 mL ethanol and then poured into the vessel containing the Na^+-MMT slurry. The mixture was stirred vigorously at 30 °C for 12 h and then allowed to cool to room temperature. The solid product was collected and washed thoroughly with deionized water to remove unreacted QX. The end product, Q-MMT, was dried at 60 °C for 24 h before analysis.

2.3. Characterization

Fourier transform infrared spectra (FT-IR) of untreated clays, QX, and modified clays were obtained using a Bruker A.M GMBH (960981(A)). The percentage nitrogen in the untreated and modified MMTs was determined using a Vario-EL III CHN Elemental Analyzer, which involved combustion in a pure oxygen environment to convert the sample elements to simple gases such as CO_2, H_2O, and N_2. Wide-angle X-ray diffraction (WXRD) with a Rigaku D/Max 2500 diffractometer with Cu-Kα radiation (40 kV, 50 mA) was used to calculate the *d*-spacing of the samples. The pore morphology of the samples was examined by high-resolution transmission electron microscopy (HRTEM) on a Jem-3010 with an accelerating voltage of 200 kV. The samples were prepared by ultrasonic dispersion, using absolute alcohol as a solvent.

Solid-state ^{27}Al MAS-NMR experiments were performed over a Bruker DSX-300 spectrometer at a frequency of 78.19 MHz. A standard 4-mm double-bearing Bruker MAS probe was used for all experiments. The nitrogen adsorption–desorption isotherms of the samples at the temperature of liquid nitrogen were measured by using a BET apparatus (Micromeritics ASAP 2020).

Table 1
Elemental analysis results of immobilized IL onto MMT.

Catalyst	CHNO from elemental analysis				N-content[a] (mmol/g)
	C (wt%)	H (wt%)	N (wt%)	O (wt%)	
MMT	0.26	1.43	0.56	9.29	–
TBA-MMT	11.64	3.18	1.08	9.86	0.77
THA-MMT	20.40	4.44	1.20	8.18	0.86
TOA-MMT	30.94	6.19	1.36	7.34	0.97
TDA-MMT	39.17	7.40	1.20	6.97	0.86

[a] Amount of ionic liquid immobilized onto MMT.

2.4. Synthesis of glycerol carbonate from glycerol and urea

In the synthesis of GC, the reaction of glycerol with urea was performed in a 50-mL *autoclave reactor* equipped with a magnetic stirrer. For each typical reaction, the Q-MMT catalyst, glycerol (50 mmol), and urea (50 mmol) were charged into the reactor. When the desired temperature was attained, the reaction was initiated by stirring under vacuum or under nitrogen purging. The products and reactants were analyzed by a gas chromatograph (HP 6890N) equipped with an FID and a capillary column (HP-5, 5% phenyl methyl siloxane). Tetraethylene glycol was used as an internal standard. The selectivity to GC was measured on the basis of glycerol as a limited reactant.

3. Results and discussion

3.1. Characterization of the Q-MMT

Elemental analysis data of MMT ion-exchanged with different tetra-alkyl ammonium chlorides (TBAC, THAC, TOAC, and TDAC) are listed in Table 1. The amount of attached QX was in the range of 0.20–0.88 mmol/g, indicating that the QX was effectively immobilized on the MMT by ion exchange. The amount of attached QX increased with an increase in the length of alkyl chains, for example, from butyl (TBA-MMT) to dodecyl (TDA-MMT), probably due to the increase in the interlayer distance of the MMT.

WXRD results for MMTs modified with ILs are presented in Fig. 1. Because the used samples were randomly oriented powders, the X-ray powder diffraction patterns showing the basal (0 0 1) reflection are one of the main identification sources for the clay group. Compared to the unmodified MMT, the *d*-spacing of the Q-MMT shifted to lower diffraction angles due to the presence of the quaternary salt. The angle 2θ shifted to the left with the increasing alkyl chain length from TBA-MMT (d) to TDA-MMT (a). As indicated in Table 2, TDA-MMT having the bulkiest cation showed the largest interlayer distance of 3.51 nm. Kim et al. [11] also reported that the *d*-spacing increased from 1.28 to 1.61 nm when a propyl group was substituted with a butyl group in the case of MMT modified with alkyl-3-methylimidazolium halide.

The N_2 adsorption–desorption isotherm for THA-MMT is shown in Fig. 2. The presence of mesopores is confirmed. The BET surface

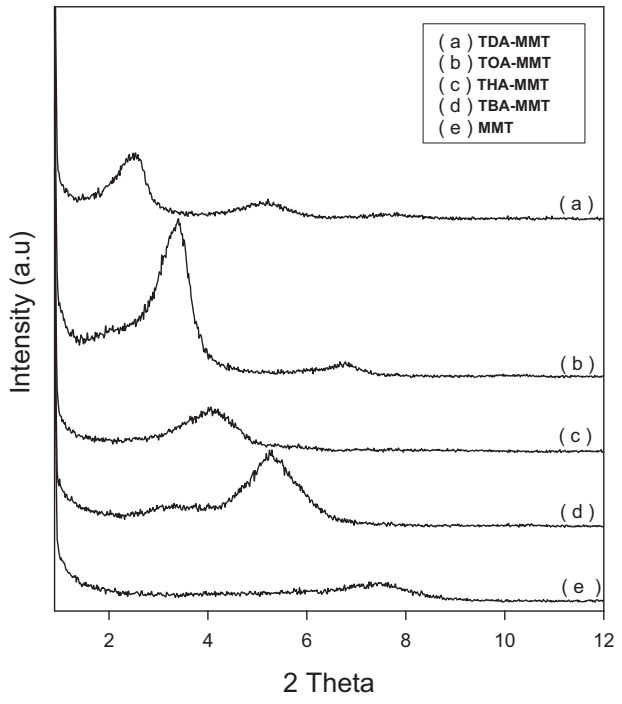

Fig. 1. X-ray diffraction of immobilized quaternary ammonium salts onto MMT.

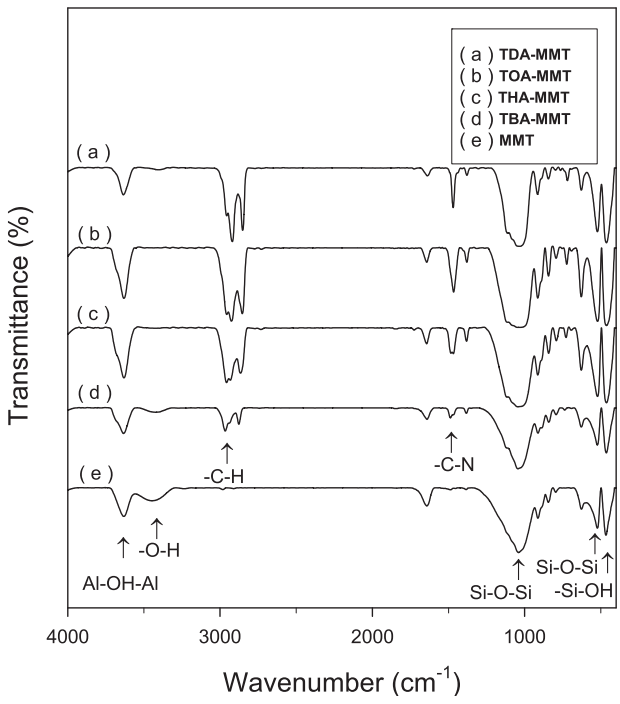

Fig. 3. FT-IR of immobilized quaternary ammonium salts onto MMT.

Table 2
Surface area and *d*-spacing of Q-MMT.

Catalyst	Surface area (m^2/g)	*d*-spacing (Å)
MMT	20.5	11.8
TBA-MMT	10.8	16.9
THA-MMT	9.7	21.9
TOA-MMT	2.8	26.0
TDA-MMT	2.6	35.1

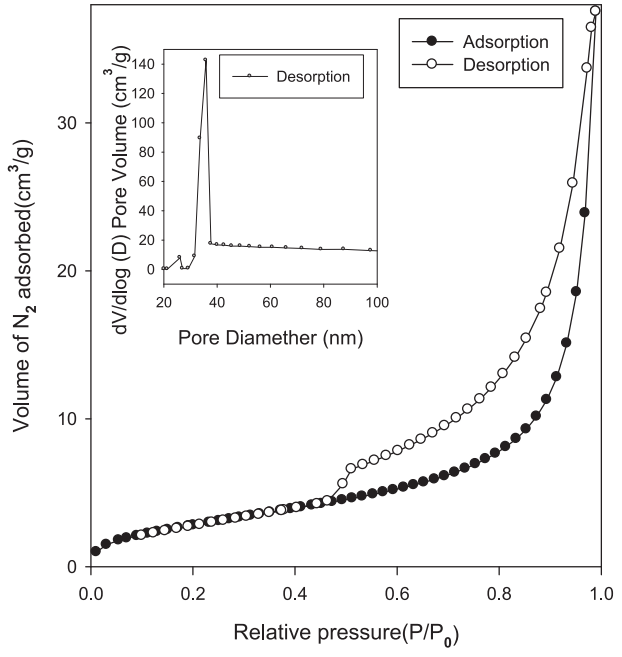

Fig. 2. N_2 adsorption–desorption isotherm for THA-MMT.

areas of the different QX-MMTs are summarized in Table 2. The initial clay MMT exhibited a surface area of 20.5 m^2/g. The surface area decreased when the quaternary salt was ion-exchanged with MMT. It decreased from 10.8 to 2.6 m^2/g with the increasing alkyl chain length from TBA-MMT to TDA-MMT, probably because the quaternary salts were bound to the clay matrix within the interlamellar space [23].

A comparison of the FT-IR spectra of unmodified MMT and Q-MMT is shown in Fig. 3. In the spectrum of MMT, the Si—O and Al—O bonds are observed at 1044 and 620 cm^{-1}, respectively. The peak at 1650 cm^{-1} and at around 3600 cm^{-1} are assigned to the bending mode of absorbed water [24] and the hydroxyl group [11], respectively. The spectrum of TDA-MMT shows peaks for the quaternary ammonium functional group in between 1000 and 1650 cm^{-1}. The peak at around 2800–3000 cm^{-1} corresponds to the long hydrocarbon chains. The infrared spectrum of TDA-MMT also shows peaks near 1460 cm^{-1} that were assigned to C—C and C—N stretching vibrations [11]. The FT-IR spectra indicate the presence of the quaternary ammonium salt in TDA-MMT.

Fig. 4 shows the $^{13}C\{H\}$ CP MAS NMR spectra of TDA-MMT (δ = 18 (l), 20–40 (b–k), 58–62 (a)). The spectrum of TDA-MMT shows peaks for the quaternary ammonium functional group in between 18 and 62 ppm. The peak at around 20–40 ppm corresponds to the long alkyl chains. The peak at 62 ppm is assigned to the carbon atoms directly adjacent to the ammonium nitrogen. The terminal carbon atoms (—CH_3) in the alkyl chain exhibited the peak at 18 ppm.

HRTEM images of MMT and TDA-MMT are shown in Fig. 5. The clay layers are indicated as solid dark lines and the pores appear in lighter contrast between the layers. The image of MMT shows that the sheets are arranged close together, and the TDA-MMT image confirms that the layered structure maintained after ion-exchange of TDA with MMT.

The ^{27}Al MAS NMR chemical shifts for MMT and Q-MMT are depicted in Fig. 6. The NMR showed two resonances at approximately 0 and 70 ppm representing Al in octahedral and tetrahedral coordination, respectively [25,26]. MMT exhibited an octahedral Al resonance at 3.1 ppm and a tetrahedral resonance at 69.9 ppm. A slight change in octahedral chemical shift was because of the

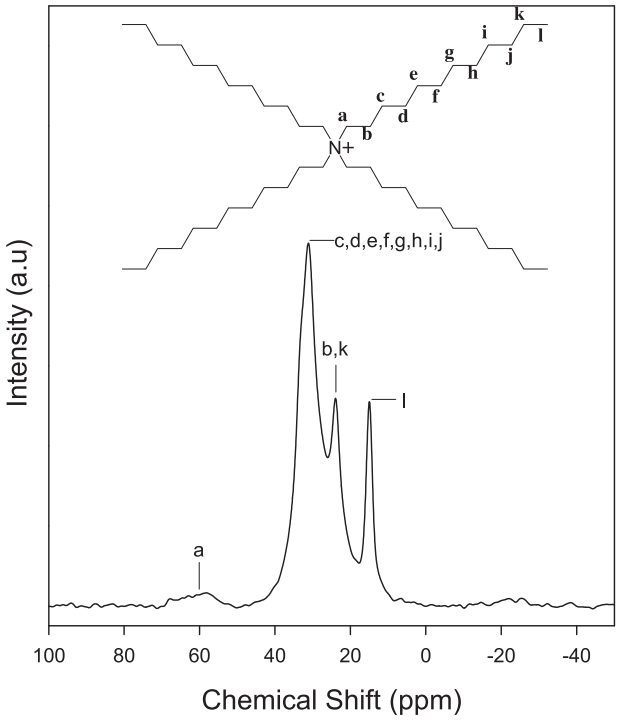

Fig. 4. Solid ^{13}C CP MAS NMR spectra of TDA-MMT.

presence of Fe [23]. Immobilization of QX onto MMT resulted in a slight shift of the tetrahedral Al peak to the right by 1.6 units, keeping the octahedral peak almost constant. Thus, during the immobilization of QX by the ion-exchange, the quaternary salts mainly interacted with the tetrahedral Al.

The X-ray photoelectron spectroscopy (XPS) results of Q-MMT are shown in Table 3. The peak of Na 1s at 1071.3 eV for MMT itself disappeared when quaternary ammonium salts were ion-exchanged with MMT, which confirms the successful ion-exchange of the quaternary cations with Na^+ ions of MMT.

Thermogravimetric analysis (TGA) curves of pure MMT and Q-MMT catalysts are shown in Fig. 7. All the Q-MMT showed good thermal stability up to 200 °C, which is much higher than the reaction temperature for the synthesis of GC from glycerol and urea. The order of thermal stability of Q-MMT is MMT > TBA-MMT > THA-MMT > TOA-MMT > TDA-MMT. The results are in general agreement with those of Awad et al. [27] where the thermal stability of trialkylimidazolium salt decreases as the length of the alkyl group attached to nitrogen increases.

3.2. Performance of Q-MMT catalysts

Despite the apparent simplicity of the reaction of glycerol with urea, this reaction can take a large number of possible pathways [28]. The accepted mechanism for the reaction involves two steps (Scheme 1): *Step 1*: The carbamoylation of glycerol to glycerol carbamate (**3**) with the liberation of one mol of ammonia. This step occurs at a higher reaction rate than the second step. *Step 2*: The carbonylation of the glycerol carbamate to GC (**4**) with elimination of a second mol of ammonia [29]. Glycerol carbamate can also produce 4-(hydroxymethyl)oxazolin-2-one (**5**) by a parallel reaction. The GC further reacts with a mol of urea to form (2-oxo-1,3-dioxolan-4-yl)methyl carbamate (**6**).

Table 3
XPS analysis of immobilized quaternary ammonium salts onto MMT.

	Binding energy (eV)				
	MMT	TBA-MMT	THA-MMT	TOA-MMT	TDA-MMT
Al2p	73.12	71.67	71.15	71.34	72.57
Na1s	1071.33	–	–	–	–
N1s	402.1	398.99	399.52	400.02	401.26
Si2p	101.37	99.39	99.07	99.25	100.52

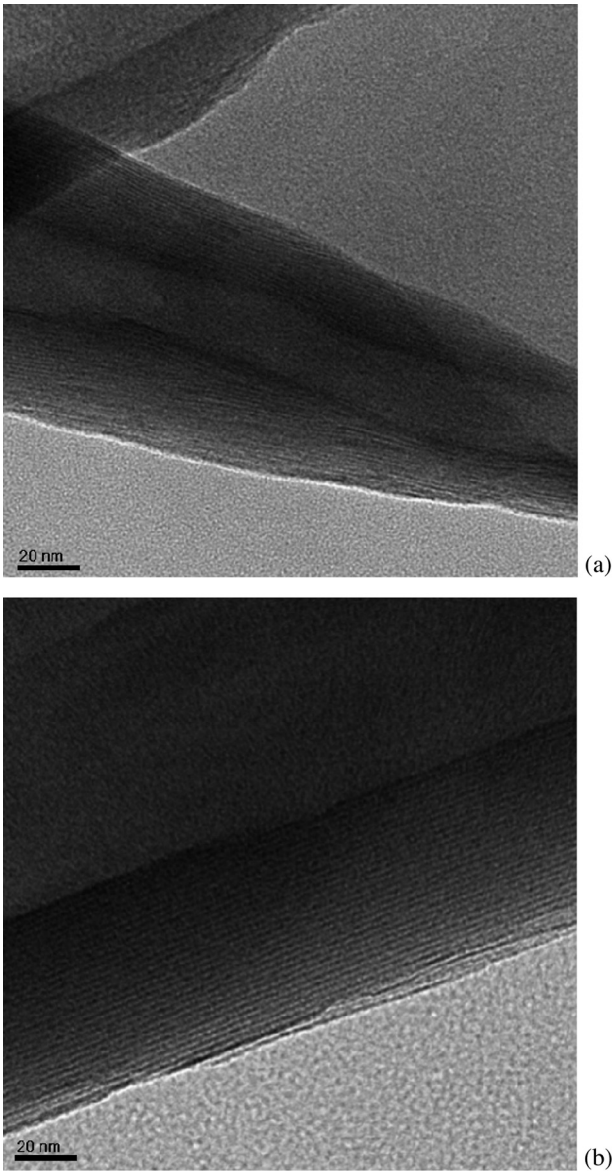

Fig. 5. HRTEM images of MMT (a) and TDA-MMT (b).

$^{13}C\{H\}$ CP MAS NMR (Fig. 8) confirmed the presence of GC, the intermediate 2,3-dihydroxypropyl carbamate (glycerol carbamate), and byproducts 4-(hydroxymethyl)oxazolin-2-one (**5**) and (2-oxo-1,3-dioxolan-4-yl)methyl carbamate (**6**).

The time-variant conversion of glycerol and the selectivity to GC and glycerol carbamate (**3**) and byproduct (**5**) and (**6**) are presented in Fig. 9 for TDA-MMT at 145 °C under a vacuum of 14.7 kPa. The conversion increased continuously up to 6 h; however, the selectivity to GC showed a maximum at 3 h and decreased at a longer reaction time due to the formation of the byproduct (**6**) by the consecutive reaction between GC and urea. The selectivity of byproduct (**5**) was less than 5%.

The conversion of glycerol, selectivity, and yield of GC for Q-MMT of different alkyl chain lengths are summarized in Table 4, under a vacuum pressure of 14.7 kPa after 3 h of reaction at 145 °C.

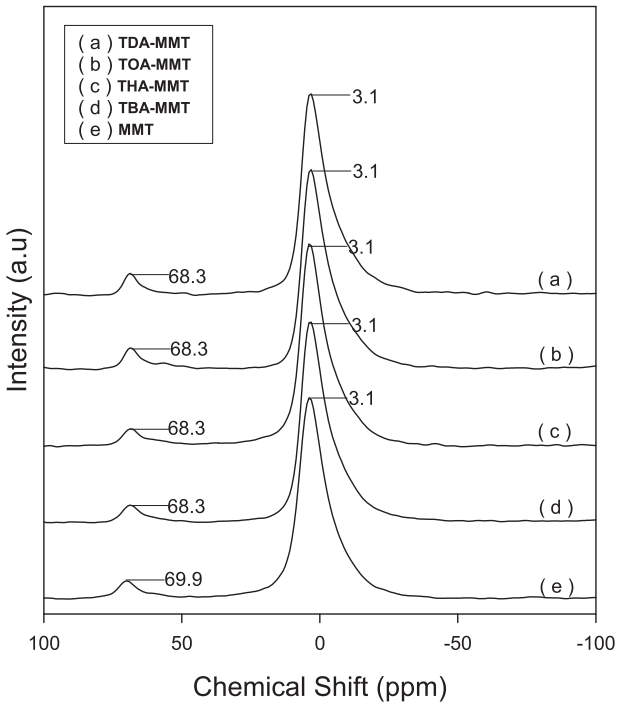

Fig. 6. Solid ^{27}Al MAS NMR spectra of immobilized quaternary ammonium salts onto MMT.

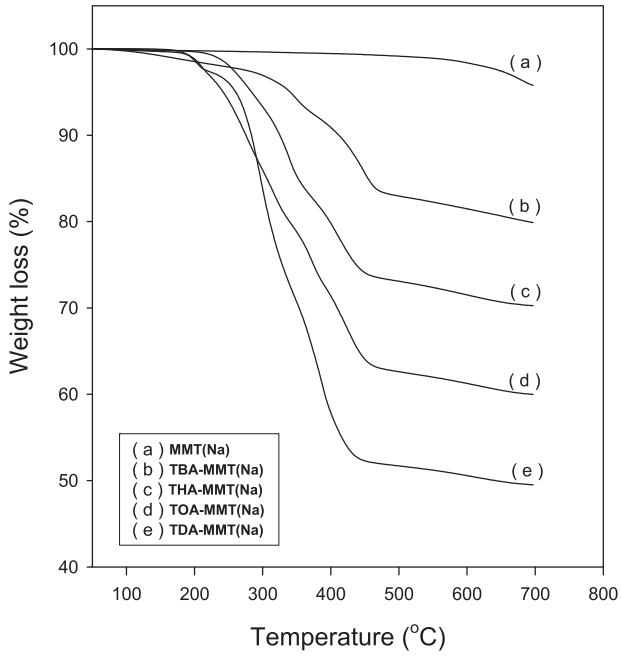

Fig. 7. Thermogravimetric analysis of immobilized quaternary ammonium salts onto MMT.

Table 4
Effects of alkyl chain structure on the reactivity of Q-MMT.

Run	Catalyst	Conversion (%)	Selectivity (%)	Yield (%)
1	TDA-MMT	53.3	78.7	42.0
2	TOA-MMT	53.2	70.8	37.7
3	THA-MMT	53.4	62.1	33.1
4	TBA-MMT	44.1	54.9	24.2
5	MMT[a]	21.6	32.5	7.0
6	TBAC[b]	52.1	54.1	28.0

Reaction conditions: glycerol = 50 mmol, urea = 50 mmol, catalyst = 0.23 g (5 wt%), reaction time = 3 h, temperature = 145 °C, degree of vacuum = 14.7 kPa.

[a] MMT = 0.23 g.

[b] TBAC = 0.18 mmol.

When the alkyl chain length changed from butyl (TBA-MMT) to dodecyl (TDA-MMT), the yield of GC also increased, because the electron-donating ability of the dodecyl group was stronger than that of the butyl group, and hence, the electron density was concentrated around the center of the active site in TDA-MMT. Increasing the bulkiness of the alkyl chain forces the oxygen anion away from the cation more easily, thereby resulting in less electrostatic interaction between the anion and the cation [30,31]. These results are in good agreement with the previous reports on the effects of the alkyl chain length [30–33]. MMT itself showed very low yield of GC. The homogeneous TBAC catalyst with equal amount of active site as TBA-MMT exhibited a little higher yield of GC than the heterogeneous TBA-MMT catalyst did.

The effects of reaction temperature on the synthesis of GC with TDA-MMT as the catalyst are shown in Fig. 10. The conversion of glycerol increased as the temperature increased from 80 to 160 °C. However, the selectivity to GC increased with temperature,

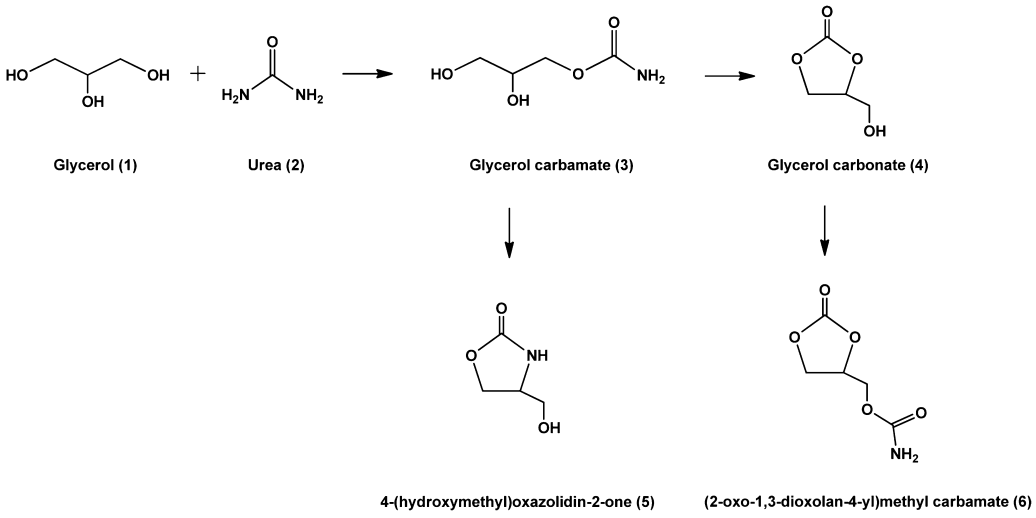

Scheme 1. Possible reaction steps for the glycerolysis of urea.

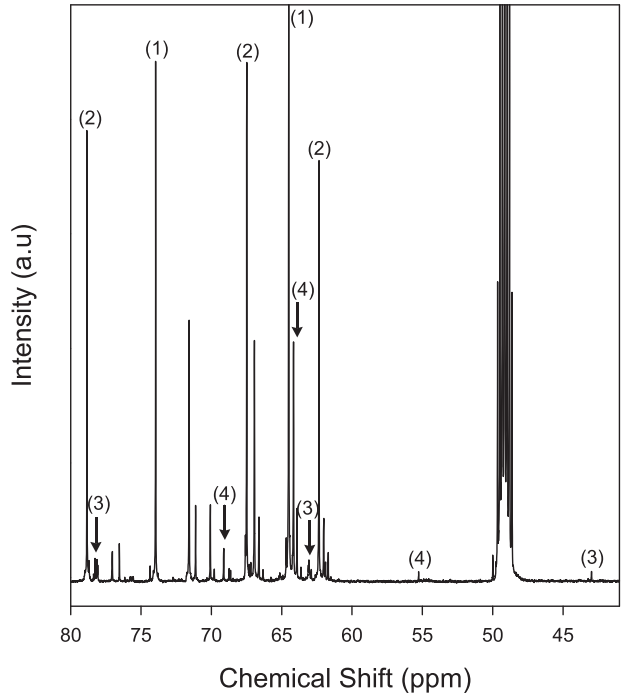

Fig. 8. ^{13}C MAS NMR spectra of the reaction mixture obtained after 3 h reaction (catalyst = 5 wt%, T = 145 °C, P = 14.7 kPa). Key: (1) = glycerol; (2) = glycerol carbonate; (3) = 4-(hydroxymethyl)oxazolidin-2-one; (4) = (2-oxo-1,3-dioxolan-4-yl)methyl carbamate. Small unlabelled peak belongs to an impurity.

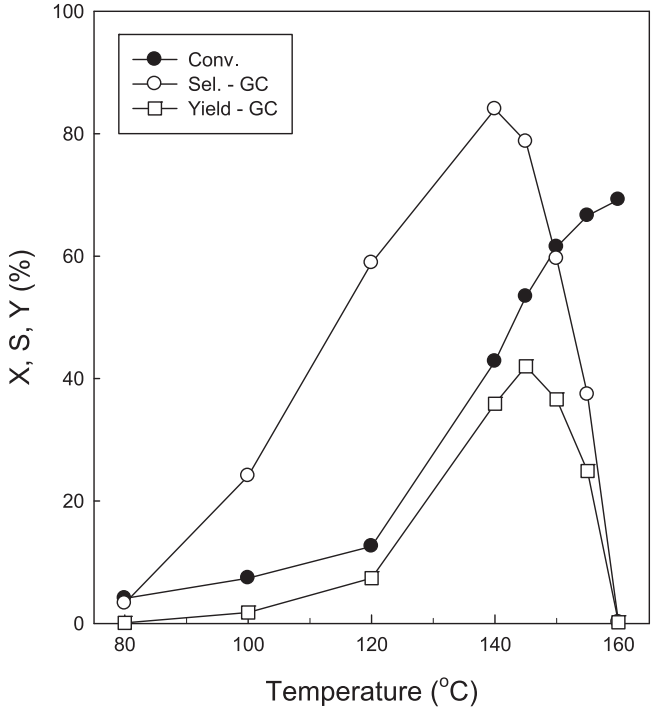

Fig. 10. The effect of reaction temperature on the synthesis of glycerol carbonate from glycerol and urea in the presence of TDA-MMT. (*Reaction conditions*: glycerol = 50 mmol, urea = 50 mmol, catalyst = 0.23 g (5 wt%), reaction time = 3 h, degree of vacuum = 14.7 kPa.)

reaching a maximum at 145 °C and decreased sharply at temperatures higher than 150 °C, probably because of the formation of (2-oxo-1,3-dioxolan-4-yl)methyl carbamate [34] or the polymerization of GC and/or glycerol.

The effects of the degree of vacuum on the reactivity of the immobilized catalyst TDA-MMT are presented in Table 5. The conversion of glycerol increased as the degree of vacuum increased from 53.3 to 3.3 kPa. A high degree of vacuum could enhance the removal of the formed ammonia gas, thereby resulting in the acceleration of the forward reaction of glycerol and urea. The selectivity to GC increased continuously when the degree of vacuum increased from 53.3 to 3.3 kPa, because a high degree of vacuum may inhibit the backward decomposition of GC to glycerol and the polymerization of GC and/or glycerol. It is also interesting to note that nitrogen purging of ammonia is as effective as operation under a high degree of vacuum. The TDA-MMT (Table 5, run 5) showed higher yield of GC than the gold-based heterogeneous catalysts at 150 °C under nitrogen flow [28].

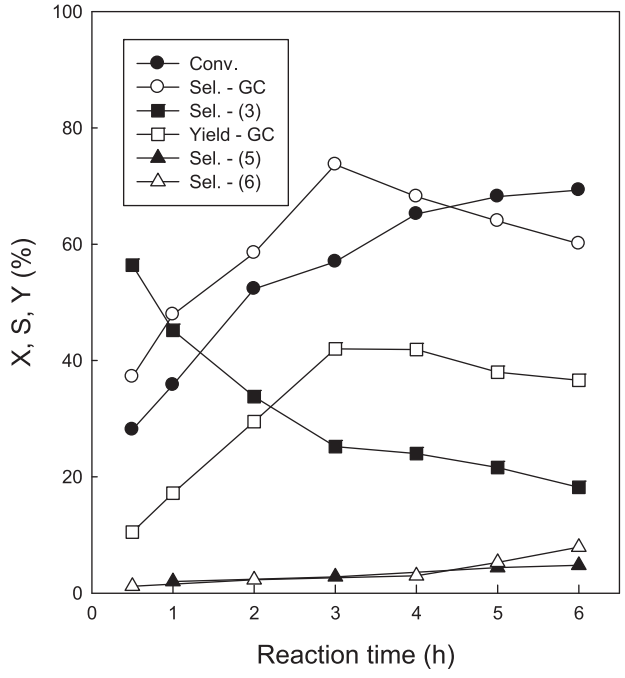

Fig. 9. The effect of reaction time on the synthesis of glycerol carbonate from glycerol and urea in the presence of TDA-MMT. (*Reaction conditions*: glycerol = 50 mmol, urea = 50 mmol, catalyst = 0.23 g (5 wt%), temperature = 145 °C, degree of vacuum = 14.7 kPa.)

The above findings together with the results of previous studies [22,28,29,35,36] suggest that the good catalysts for the reaction between glycerol and urea should possess both Lewis acidity and basicity, for the activation of carbonyl group of urea and hydroxyl group of glycerol, respectively. In this regards, for the reaction of glycerol and urea with Q-MMT catalysts, Lewis acidic quaternary ammonium cation can activate the urea and Lewis basic oxygen anion in the MMT activate the glycerol. The role of the quaternized functional group in the glycerolysis of urea was proposed by Park et al. [35], who used FT-IR and ^{1}H NMR analysis to demonstrate that there were strong hydrogen bonding interactions between

Table 5
Effects of pressure on the reactivity of TDA-MMT.

Run	Degree of vacuum (kPa)	Conversion (%)	Selectivity (%)	Yield (%)
1	3.3	59.1	79.0	46.7
2	14.7	53.3	78.7	42.0
3	26.6	50.2	67.7	34.0
4	53.3	48.4	54.3	26.3
5	N_2 purge (150 mL/min)	57.9	81.2	47.0

Reaction conditions: glycerol = 50 mmol, urea = 50 mmol, catalyst = 0.23 g (5 wt%) TDAC-MMT, reaction time = 3 h, temperature = 145 °C.

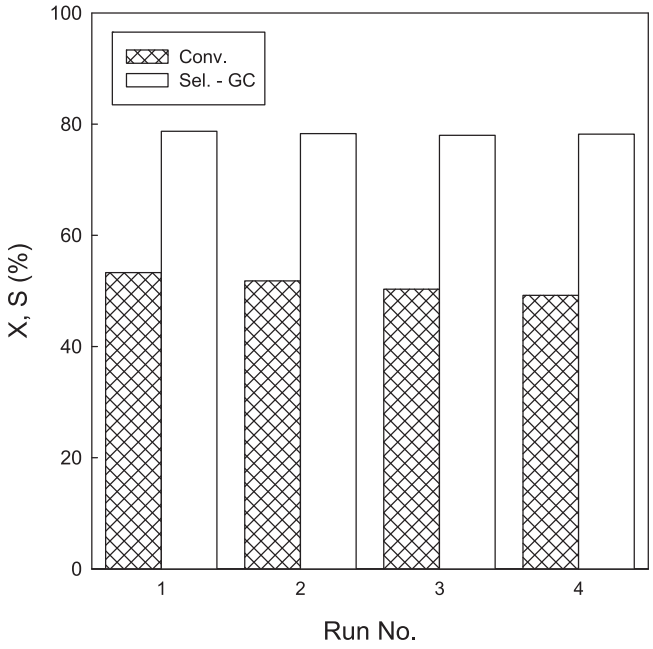

Fig. 11. Recycle test of TDA-MMT. (*Reaction conditions*: glycerol/urea molar ratio = 1, catalyst = 5 wt%, reaction time = 3 h, temperature = 145 °C, degree of vacuum = 14.7 kPa.)

the hydroxyl group of glycerol and the chloride anion of NH_4Cl. However, Fujita et al. [36] reported a homogeneous reaction mechanism for solid zinc catalysts, where a complex of a Zn atom coordinated with N═C═O was considered as the active species of the glycerolysis of urea. Therefore, for heterogeneous catalysts, the role of the support should be further studied more in detail for the illumination of the exact reaction mechanism.

Recycling experiments were performed to investigate the stability of the Q-MMT. In each cycle, the used catalyst was separated by filtration, washed with methanol to remove the products adhering to the surface of catalyst, dried at room temperature, and then reused directly for the next run without regeneration. The activity of the reused Q-MMT catalyst is shown in Fig. 11. Although the conversion of glycerol decreased slightly, the selectivity to GC was almost the same as before. This indicates that the catalyst can be reused at least up to four consecutive times without any considerable loss of its activity.

4. Conclusions

Quaternary ammonium salts were successfully immobilized onto MMT through ion-exchange reaction. In the synthesis of GC from glycerol and urea, Q-MMT showed good catalytic performance even in the absence of any solvent. Q-MMT with long alkyl chain structures exhibited better reactivity for the synthesis of GC. High temperature, long reaction time, and a high degree of vacuum were favorable for the high conversion of glycerol. Q-MMT can be easily recovered and reused without any considerable loss of their initial activity.

Acknowledgments

This study was supported by the National Research Foundation (2012-001507) of Korea, Global Frontier Program and the Brain Korea 21 PLUS.

References

[1] G. Knothe, J. Van Gerpen, J. Krahl (Eds.), The Biodiesel Handbook, AOCS Press, Champaign, IL, 2005.
[2] S.T. Bagley, L.D. Gratz, J. Johnson, J. McDonald, Environ. Sci. Technol. 32 (1998) 1183–1191.
[3] M. Mittelbach, C. Remschmidt, Biodiesel – The Comprehensive Handbook, Karl-Franzens University, Graz, Austria, 2004.
[4] T. Werpy, G. Petersen, Top Value Added Chemicals from Biomass, vol. 1, US Department of Energy (USDOE), 2004.
[5] M. Aresta, A. Dibenedetto, F. Nocito, C. Ferragina, J. Catal. 268 (2009) 106–114.
[6] D. Randall, R. De Vos, Eur. Pat. EP 419114 (1991).
[7] M. Weuthen, U. Hees, Ger. Pat. DE 4335947 (1995).
[8] Q. Li, W. Zhang, N. Zhao, W. Wei, Y. Sun, Catal. Today 115 (2006) 111–116.
[9] M. Okutsu, T. Kitsuki, JP 2007039347 (2007).
[10] M. Aresta, J.L. Dubois, A. Dibenedetto, F. Nocito, C. Ferragina, EP 08305653.1 (2008).
[11] N.H. Kim, S.V. Malhotra, M. Xanthos, Microporous Mesoporous Mater. 96 (2006) 29–35.
[12] K.V. Bineesh, D.K. Kim, M.I. Kim, M. Selvaraj, D.W. Park, Dalton Trans. 40 (2011) 3938–3945.
[13] E. Ruiz-Hitzky, P. Aranda, J.M. Serratosa, in: M. Auerbach, K. Carrado, P.K. Dutta (Eds.), Handbook of Layered Materials, Marcel Dekker, New York, 2002, pp. 91–154.
[14] H. He, J. Duchet, J. Galy, J.F. Gerald, J. Colloid Interface Sci. 295 (2006) 202–208.
[15] S.Y. Lee, W.J. Cho, K.J. Kim, J.H. Ahn, M. Lee, J. Colloid Interface Sci. 284 (2005) 667–673.
[16] D.W. Kim, D.K. Kim, M.I. Kim, D.W. Park, Catal. Today 185 (2012) 217–223.
[17] T. Welton, Chem. Rev. 99 (1999) 2071–2083.
[18] P. Wasserscheid, T. Welton, Ionic Liquids in Synthesis, 2nd ed., Wiley-VCH, Weinheim, 2008.
[19] H.Y. Ju, M.D. Manju, K.H. Kim, S.W. Park, D.W. Park, J. Ind. Eng. Chem. 14 (2008) 157–160.
[20] M.D. Manju, J.I. Yu, J.Y. Ahn, D.W. Park, Green Chem. 11 (2009) 1754–1757.
[21] H.J. Cho, H.M. Kwon, J. Tharun, D.W. Park, J. Ind. Eng. Chem. 16 (2010) 679–683.
[22] D.W. Kim, M.S. Park, M. Selvaraj, G.A. Park, S.D. Lee, D.W. Park, Res. Chem. Intermed. 37 (2011) 1305–1312.
[23] G. Sanjay, S. Sugunan, J. Porous Mater. 15 (2008) 359–367.
[24] M. Gustavo, D. Nascimento, V.R.L. Constantino, R. Landers, M.L.A. Temperini, Macromolecules 37 (2004) 9373–9385.
[25] R. Jelinek, B.F. Chmelka, A. Stein, G.A. Ozin, J. Phys. Chem. 96 (1992) 6744–6752.
[26] Q. Liu, D.A. Spears, Q. Liu, Appl. Clay Sci. 19 (2001) 89–94.
[27] W.H. Awad, J.W. Gilman, M. Nyden, R.H. Harris, T.E. Sutto Jr., J. Callahan, P.C. Trulove, H.C. DeLong, D.M. Fox, Thermochim. Acta 409 (2004) 3–11.
[28] C. Hammond, J.A. Lopez-Sanchez, M.H. Ab Rahim, N. Dimitratos, R.L. Jenkins, A.F. Carley, Q. He, C.J. Kiely, D.W. Knight, G.J. Hutchings, Dalton Trans. 40 (2011) 3927–3937.
[29] M.J. Climent, A. Corma, P. De Frutos, S. Iborra, M. Noy, A. Velty, P. Concepcion, J. Catal. 269 (2010) 140–149.
[30] L. Han, S.W. Park, D.W. Park, Energy Environ. Sci. 2 (2009) 1286–1292.
[31] H.L. Shim, S. Udayakumar, J.I. Yu, I. Kim, D.W. Park, Catal. Today 148 (2009) 350–354.
[32] H. Kawanami, A. Sasaki, K. Matsui, Y. Ikushima, Chem. Commun. 7 (2003) 896–897.
[33] S.S. Wu, X.W. Zhang, W.L. Dai, S.F. Yin, W.S. Li, Y.Q. Ren, Appl. Catal. A: Gen. 341 (2008) 106–111.
[34] H. Ceri, A.L.S. Jose, H.A.R. Mohd, D. Nikolaos, L.J. Robert, F.C. Albert, H. Qian, J.K. Christopher, W.K. David, J.H. Graham, Dalton Trans. 40 (2011) 3927–3937.
[35] J.H. Park, J.S. Choi, S.K. Woo, S.D. Lee, M. Cheong, H.S. Kim, H. Lee, Appl. Catal. A: Gen. 433 (2012) 35–40.
[36] S.I. Fujita, Y. Yamanishi, M. Arai, J. Catal. 297 (2013) 137–141.